

## RESEARCH ARTICLE

# Data-Driven Modeling of Aero-Engine Performance Degradation Models

MINGYANG ZHOU<sup>1,2,3</sup>, KEQIANG MIAO<sup>2,3</sup>, JIAXIAN SUN<sup>2,3</sup>, YAFENG SHEN<sup>2,3</sup>, AND BO HAN<sup>2,3</sup>

<sup>1</sup>University of Chinese Academy of Sciences (UCAS), Beijing 100049, China

<sup>2</sup>Institute of Engineering Thermophysics, Chinese Academy of Sciences, Beijing 100089, China

<sup>3</sup>National Key Laboratory of Science and Technology on Advanced Light-duty Gas-turbine, Beijing 100089, China

Corresponding author: Keqiang Miao (miukeqiang@iet.cn)

This work was supported by CAS Strategic Pilot Project for Key and Core Technologies, under Grant XDC0143000.


**ABSTRACT** Periodic maintenance is a fundamental method of aero engine maintenance. However, frequent regular maintenance leads to resource wastage and inefficient maintenance. With the increasing technological maturity, integration, and complexity of aero engines, the costs of research and development are rising, creating an urgent demand for advanced Prediction and Health Management technology (PHM). PHM technology enables the transition from periodic maintenance to predictive-based maintenance by modeling aero-engine performance degradation, thereby allowing for life prediction and sensor parameter prediction. Data-driven modeling methods have gained popularity owing to their strong traceability, wide consideration range, and high freedom of adjustment; however, they currently suffer from low prediction accuracy and reliability. To address this issue, this study utilizes NASA's open data set C-MAPSS for data preprocessing before inputting it into the LSTM training network to obtain function loss values in the forward direction. These values are then updated through the quantum particle swarm algorithm to achieve loss reduction optimization of key parameters to obtain the best QPSO-LSTM aero-engine performance degradation model. Additionally, the PCA method was used for dimensionality reduction modeling by calculating variance percentages of data eigenvalues which determined 11 dimensions as the lowest dimension for progressive reduction modeling. Ultimately, it was found that the QPSO-LSTM combined neural network remaining life prediction achieved a minimum RMSE value of 22.04, which is 43.76% higher than that of the basic model, presenting an excellent linear fitting relationship after crossing threshold values despite not conforming initially with true value trends at initial time nodes.

**INDEX TERMS** Data-driven, aeroengine, long short-term memory network, particle quantum swarm algorithm.

## I. INTRODUCTION

Aero-engines are always in an extreme working environment of high temperature, high pressure and high rotational speed in the process of performing flight missions, which leads to blade wear or blade gap enlargement due to unexpected factors and its own long-time high-speed rotation, resulting in a decrease in the efficiency of the pressurizer inside the engine, and then recruits the engine performance degradation. Aero-engine performance degradation modeling based on

aero-engine data is the basis for solving problems related to the prediction of scenario-based maintenance [1], where the model's merit directly determines the upper limit of the problem-solving capability, while the data is the lower limit of the problem-solving requirements. In addition, the model and data are key elements in realizing the PHM technology of aero-engines. Among the many existing performance degradation modeling approaches for aero-engines, data-driven performance degradation modeling has the advantages of strong traceability, a wide range of considerations, a high degree of freedom of adjustment, and excellent development prospects. Data-driven aero-engine performance degradation

The associate editor coordinating the review of this manuscript and approving it for publication was Zhenbao Liu .

models mainly include statistical and artificial intelligence models. Compared with statistical models, artificial intelligence models have gradually become the mainstream modeling method for aero-engine performance degradation models in recent years, owing to their outstanding ability to deal with nonlinear data and the advantage of forming a more reliable model by dealing with huge amounts of data [2].

Artificial intelligence algorithms perform performance degradation modeling without the need for a specific degradation model as in the case of statistical algorithms. Instead, they simulate the performance degradation process through label training and feature extraction. As the processing depth of the problem in question increases and larger scale data floods into the traditional AI algorithms, the traditional AI algorithms represented by shallow machine learning algorithms begin to show their decline [3]. At this time, deep learning algorithms based on shallow AI algorithms have come to the fore. The model established by such algorithms realizes the automatic extraction of features into information that can be recognized by computers through unusually complex transformations, which not only greatly reduces the manual workload, but also shows better results in systems with more data, and has become the focus of research in recent years. In the aero-engine performance degradation model, the scale of data to be processed far exceeds the strong range of traditional artificial intelligence algorithms; therefore, deep learning models come first in the imperial examinations progressively in such problems.

The use of LSTM models to address the modeling of aero-engine performance degradation models, although currently demonstrating promising accuracy and generalization capabilities, still has the following pain point issues that need to be addressed:

- A single LSTM model has a limited extraction capability for optimization parameters, which makes it difficult to achieve the expected results of the model. Although sections of the research methods utilize some performance extraction tools to construct optimized LSTM models, the small volume of aforesaid research and certain requirements on data dimensions and quality lead to limited final results of the models.
- There is insufficient consideration of the data preprocessing in the C-MAPSS dataset. Data in the C-MAPSS dataset inevitably introduces erroneous points, redundancy points, and measurement noise. Inadequate filtering leads to excessive invalid data in the model, which results in a severely impaired model. Excessive filtering, in turn, leads to a loss of good data, again affecting model performance. Effective filtering of data is understudied in current studies, and models in most studies fail to achieve the desired results; thus further research is required.

This study attempts to optimize the LSTM model with the QPSO algorithm to achieve better parameter adjustment; and to select the open commercial modular aero-propulsion

system simulation dataset of NASA as the data source. At the same time, the dataset is downsampled to obtain lower RMSE (Root Mean Square Error) values for remaining life prediction, and the optimal model parameter combinations are sought through the specific data on the one hand, while high-fitting aero engine performance degradation modeling is obtained. The above work aims to provide technical support for data-driven aero-engine performance degradation modeling.

## II. RELATED WORKS

An integrated Deep Belief Nets (DBN) based on the time accumulation problem has been proposed to achieve a highly robust aero-engine performance degradation model, thus realizing the assessment of aero-engine reliability [4]. The DBN network has been used while incorporating the dynamic learning rate in the process of solving the mechanical equipment performance degradation model, which, to a certain extent, avoids the problem of poor convergence of the model [5]. The DBN model of high-reliability mechanical equipment successfully validated its performance. To improve the applicability of the model, an autoencoder (AE), an excellent feature compression and extraction tool, was used on top of the DBN model has been performed to optimize the parameters of the model, thus improving the effectiveness of the model [6]. In addition to the use of autoencoders, some scholars have used other machine learning models for DBN parameter model optimization. For example, the Particle Swarm Optimization (PSO) algorithm has been used in the DBN model, resulting in a DBN model with better robustness than shallow machine learning models [7]. Convolutional Neural Networks (CNN) and Transformer Neural Networks based on the attention mechanism are frequently used algorithmic models for the establishment of mechanical equipment performance degradation models. The subsequent research realized the establishment of a high-reliability aero-engine performance degradation model by bringing multivariate time series samples and corresponding performance degradation quantities into a unidimensional input CNN network [8]. The convolution kernel was utilized to extract the significant features of the sequence, and it was verified that the model has a higher prediction accuracy than the traditional CNN through the C-MAPSS dataset [9]. After years of research, scholars have found that the CNN model can not only automatically extract features; but also filter itself, which has a full development prospect.

RNN, as an algorithm specialized in processing time series data for correlation prediction, is highly relevant to the performance degradation problem of aero-engines. With the deepening of the research, scholars have found that in the process of modeling using RNN, there are defects of gradient disappearance or gradient explosion, which leads to the key features of the more distant time nodes being forgotten in the current time period, resulting in a training effect that falls short of expectations. LSTM, or a Long Short-Term

Memory Model, was created as a result of this, which is a traditional RNN structure with the addition of a forgetting gate to realize long-and short-term memory by means of the gate control system. Weight values; that solve the pain point problem in traditional RNN models. The Variational Autoencoder (VAE) tool in LSTM was used to improve the feature collection ability of the network, and the model was verified through various public datasets such as PHM08 for analysis. The experimental results were more reliable and practical [10]. A researcher found that the conventional LSTM model has the problem of not being able to have strong generalization ability under multiple operating conditions and faults; therefore, they constructed a bidirectional LSTM network to establish an aero-engine performance degradation model and applied the LSTM to the model [11].

### III. INITIALLY MODELING

#### A. IDEA FOR MODELING

The modeling ideas in this chapter are as follows. First, data analysis and preprocessing are carried out to determine the final serial number of sensors that need to be processed, and the noise together with obvious error data in the signal are filtered. Second, after dimensionality reduction and normalization, the dataset was imported into the LSTM network for training. Finally, the loss values computed through the LSTM training process are reversed input and updated using the QPSO algorithm. The design framework of the QPSO-LSTM-based performance degradation prediction model is illustrated in Fig.1.

#### B. PRE-TRAINING OF DATA

##### 1) DATA ANALYSIS

Among the four sub-datasets of C-MAPSS, the FD001 dataset has a single operating condition and a clear fault state. Considering the high data stability, this training set is used as an example for modeling in this chapter. The FD001 sequential data is divided into two sets of data; a test set and a training set. The dimensions of each dataset is 26, which consists of the engine number, number of operating cycles, three operation settings, and 21 sets of sensor data [12].

Among them, seven sets of sensor data remain constant during the simulation run: S1, S5, S6, S10, S16, S18, and S19 sets of data, which are always equal to the initial state values and do not change with an increase in the number of engine operating cycles. For example, the S1 data correspond to the total fan inlet temperature, which means that the airflow is completely stagnant, that is, the temperature of the fan inlet when the speed is 0, and it will not change with the change in the engine state.

##### 2) SELECTION OF CHARACTERISTIC PARAMETERS

Not all airway parameters in the sensor data of the C-MAPSS dataset are associated with engine performance degradation; therefore, a parameter correlation analysis is required to determine the ordinal numbers of data that are meaningfully

associated with aero-engine performance degradation. In this section, the Pearson product-moment correlation coefficient is selected for parameter correlation analysis, while the results of the calculation are applied as a guide for parameter selection.

Pearson's correlation coefficient is commonly used to indicate the degree of correlation between variables and takes values within the interval  $[-1,1]$ , which is defined by the following formula:

$$\rho_{X,Y} = \frac{\text{cov}(X, Y)}{\sigma_X \sigma_Y} = \frac{E[(X - \mu_X)(Y - \mu_Y)]}{\sigma_X \sigma_Y} \quad (1)$$

where  $\rho$  denotes the overall correlation coefficient,  $\sigma$  is the standard deviation,  $E$  is the mean, and  $\text{cov}(X,Y)$  is the covariance between  $X$  and  $Y$ . With the covariance and standard deviation, the Pearson's correlation coefficient  $r$  can be calculated using the following formula:

$$r = \frac{1}{n-1} \sum_{i=1}^n \left( \frac{X_i - \bar{X}}{\sigma_X} \right) \left( \frac{Y_i - \bar{Y}}{\sigma_Y} \right) \quad (2)$$

The correlation between  $X$  and  $Y$  is determined by  $\rho_{X,Y}$ . The larger  $\rho_{X,Y}$  is, the more correlated  $X$  and  $Y$  are. Conversely, the smaller  $\rho_{X,Y}$  is, the less correlated  $X$  and  $Y$  are. In addition the coefficient does not change by changing the size of the variable [13].

The sensor data were imported, and a heat map of the Pearson's correlation coefficient was plotted, as shown in Fig.2.

The constant sequences S1, S5, S10, S16, S18, and S19 are shown to be non-numeric, implying no correlation with the other data; therefore, they are considered noise and processed for data rejection to prevent the additional burden of aggravating the computation during the subsequent training process. The data of S6, on the other hand, show a weak correlation with other parameters, although it is a constant sequence, so this sequence data is remained. Among the other 14 sets of data other than the constant sequence, the data of S7, S12, S20 and S21 show an obvious correlation with the number of operating cycles, whereas the other sequences of sensor signals are partly positively correlated and partly negatively correlated, and display insignificant regularity with the number of cycles. In summary, data S2, S3, S4, S6, S7, S8, S9, S11, S12, S13, S14, S15, S17, S20, and S21 were selected for the subsequent modeling work in this chapter.

##### 3) NORMALIZATION

Based on the complex operating conditions of aero engines, noisy data and anomalous data points are inevitably generated during the information transfer process; hence, to improve the modeling efficiency, the data set needs to be filtered. Shift smoothing filtering is a smoothing algorithm that specifies a sliding window and calculates the mean value thereof. It is commonly used to reduce the noise in the signal or remove the high-frequency components in the prediction problem, thus smoothing the signal.

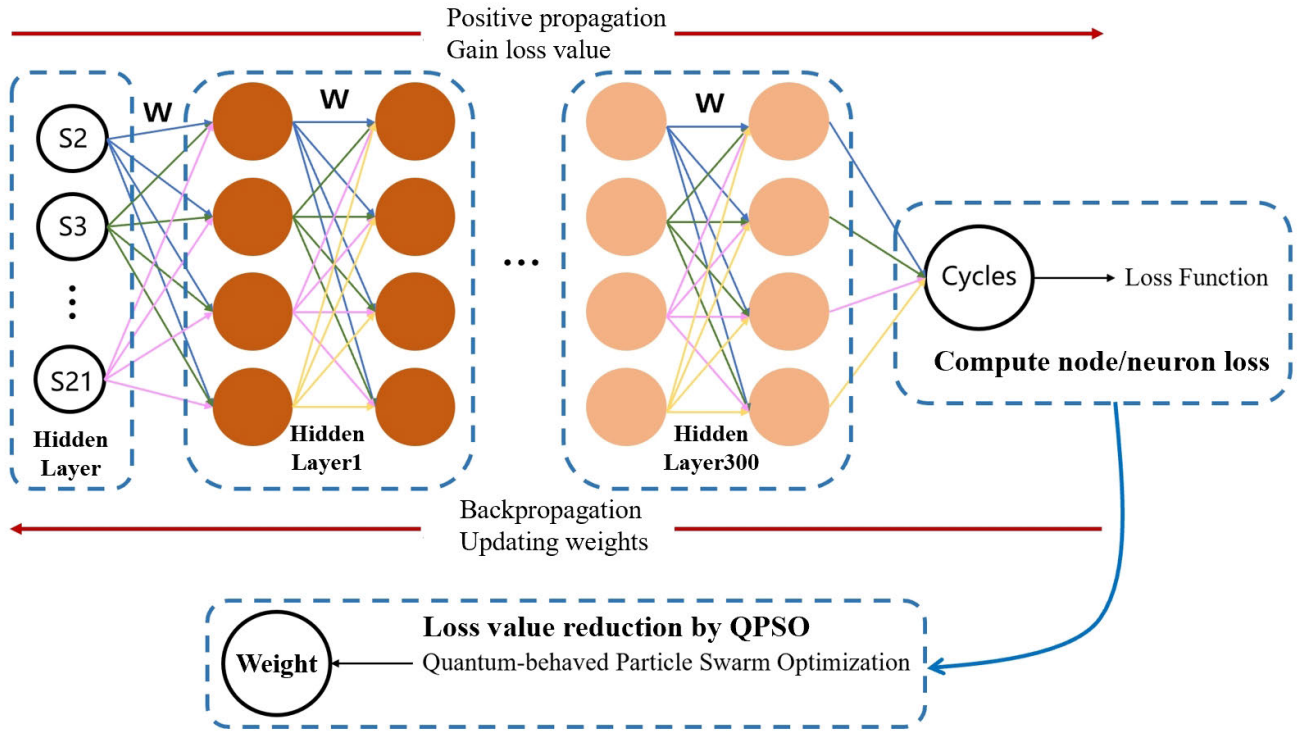


FIGURE 1. QPSO-LSTM predictive modeling design framework.

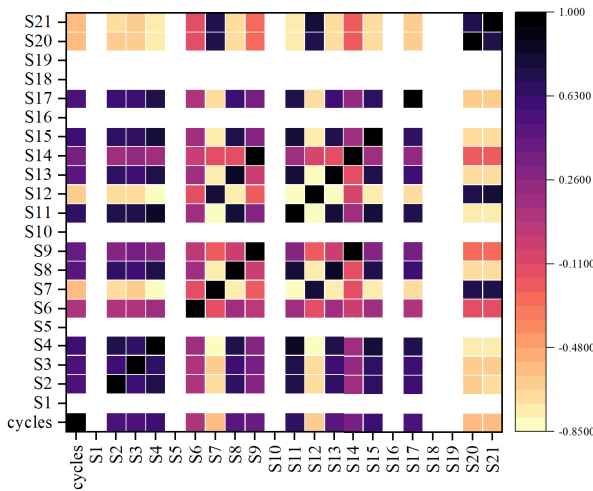


FIGURE 2. Heat map of Pearson's correlation coefficient.

The basic principle is as follows: supposing that there is a sequence  $Y = (y(1), y(2), \dots, y(n))$ , then the noise reduction formula is:

$$x(t) = \frac{y(t) + y(t-1) + \dots + y(t-s+1)}{s} \quad (3)$$

In the formula,  $x(t)$  is the smoothed value, and  $s$  is the window length. The final sequence of true values after noise reduction was obtained  $X = (x(1), x(2), \dots, x(n))$ . Excessive smoothing

can cause the data to lose its realism; therefore, the window length is set to four in this chapter.

#### 4) FILTERING

The data normalization method used in this chapter is Z-score normalization, or standard deviation normalization, which calculates the difference between the sample and the population. The method takes the original data mean and standard deviation as parameters; and converts the original data into a new function that conforms to the standard normal distribution and is dimensionless, thus maintaining the comparability of the data [14].

The formula for Z-Score standardization is:

$$x_{\text{normalization}} = \frac{x - \mu}{\sigma} \quad (4)$$

where  $x$  denotes the initial data,  $\mu$  the initial data mean, and  $\sigma$  the initial data standard deviation.

### C. QPSO-LSTM NETWORK CONSTRUCTION

In this chapter, the seven constant sequence data in the C-MAPSS dataset were first eliminated, and after the parameter correlation calculation, the sequence S6, which showed low correlation with other parameters, was retained. The data S2, S3, S4, S6, S7, S8, S9, S11, S12, S13, S14, S15, S17, S20, and S21 were finally selected as the model, and the data source was imported into the training network.

The construction of the LSTM training network includes data import and preprocessing, setting of hidden and fully



connected layers, setting of iteration number and training batch size, optimizer selection, setting of the maximum number of training sessions and minimum batch size, setting of the learning rate and validation period, training of the network, and output of the results. The specific parameter settings of the LSTM are listed in Table 1, and Table 2 lists the QPSO algorithm parameter settings.

**TABLE 1.** Key parameter settings of LSTM.

Key Parameters	Setting
Hardware Device	Single-CPU
Hidden Layer	300
Full Connected Layer	152
Iteration Number	50
Training Batch	5000
Optimizer	Adam
Learning Rate	0.001
Validation Cycle	10

**TABLE 2.** Key parameter settings of QPSO.

Key Parameters	Setting
Initial Population Size	3
Space Dimension	2
Maximum Number of Iterations	10
Position Parameter Setting	[100,300]

## D. RESULTS

### 1) SCORING STANDARD

In this chapter, the Root Mean Square Error (RMSE) is chosen to evaluate the life prediction results, which is a measure of the predictive accuracy of a predictive model on continuous data; that quantifies the root-mean-square difference between the predicted values and the actual values [15]. RMSE, as a measure of the mean deviation between the predicted values and true results, is a commonly used performance evaluation metric in regression tasks one of them.

Its calculation formula is:

$$\text{RMSE} = \sqrt{\frac{1}{N} \sum_{i=1}^N h_i^2} \quad (5)$$

In the above equation,

$$h_i = \text{RUL}'_i - \text{RUL}_i \quad (6)$$

N represents the total number of engines and i represents the number of engines. RUL' represents the predicted value of RUL, whereas RUL represents the true value. The smaller the RMSE value, the better the prediction.

### 2) RUL PREDICTION RESULTS

After three steps of data preprocessing, LSTM model building and QPSO algorithm optimization, the aero-engine life prediction results and optimization prediction results based on the subset of the C-MAPSS dataset FD001 were

obtained. The prediction results are shown in Fig.3, and the real values of the remaining engine life, LSTM network prediction results, QPSO-LSTM optimization prediction results are represented by blue straight lines, orange dashes, and green long dashes, respectively.

As shown in Fig.3, the QPSO algorithm is generally effective in optimizing the first 20 groups of engines and is more effective in optimizing the remaining engine life prediction results after 20 groups. Overall, the root mean square error (RMSE) of the remaining life prediction results of the LSTM network was 38.57, and the RMSE of the QPSO-LSTM optimized network was 32.75. Compared with the unoptimized RUL prediction results, the RUL prediction results of the network optimized by the QPSO algorithm were improved by approximately 15%.

### 3) SCORING STANDARD

A data-driven approach for modeling performance degradation requires the identification of RUL output labels. Owing to the pre-operational stage of the engine, the components are running well, performance degradation can be disregarded at this stage, and the aero-engine is in a healthy operational state. The failure moment of the full life cycle of the aero-engine can be regarded as RUL = 0. When it is greater than or equal to the threshold value, the RUL is a constant value; when it is less than the threshold value, the RUL decreases linearly with the cycle. In this section, a segmented function is used to represent the performance-degradation curve. When the remaining service life is greater than or equal to the threshold value, the RUL is a constant value, and when the remaining service life is less than the threshold value, the RUL decreases linearly with the cycle until the engine fails. In the literature the remaining service life threshold is generally set between 120 and 130, and in this chapter 125 is taken as the RUL labeling threshold [2]. Furthermore, the performance degradation model is established by taking the engine NO.2 in the FD001 subset of the C-MAPSS dataset as an example, and its performance degradation model is shown in Fig.4.

As can be seen in Fig.4, the performance degradation model initially established by the combined QPSO-LSTM model fits the engine degradation model established using the segmented linear method, although it presents a better fit in the middle section and shows an obvious slope slowing down in the interval of the remaining life threshold from 120 to 130. However, the change in the poles at both ends presents the engine degradation trend in general. Further dimensionality reduction of the dataset is required to establish a more reliable degradation model for aero-engine performance.

## IV. DIMENSIONALITY REDUCTION FOR SEARCHING SUPERIORITY

### A. GAUGE FOR DIMENSIONALITY REDUCTION

The performance of a neural network can fluctuate erratically with changes in a dataset. In this chapter, for example,

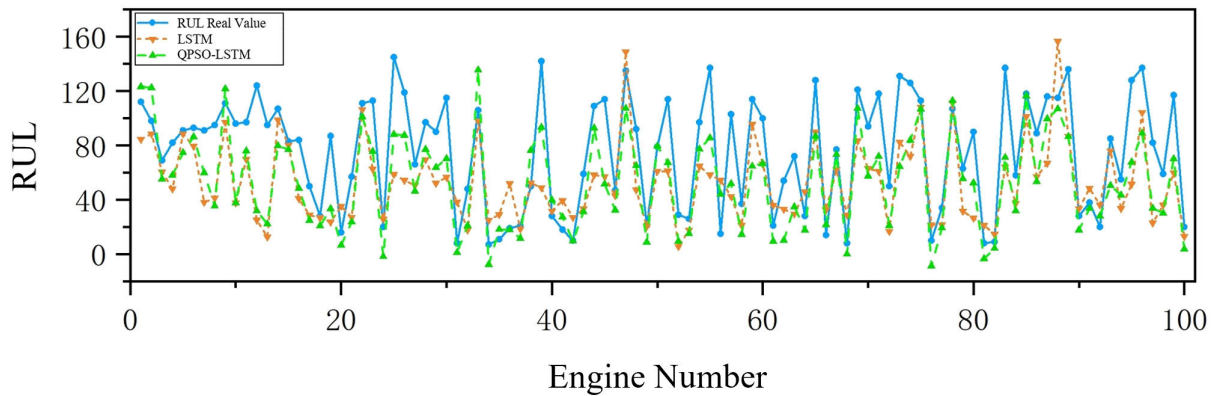


FIGURE 3. RUL prediction results.

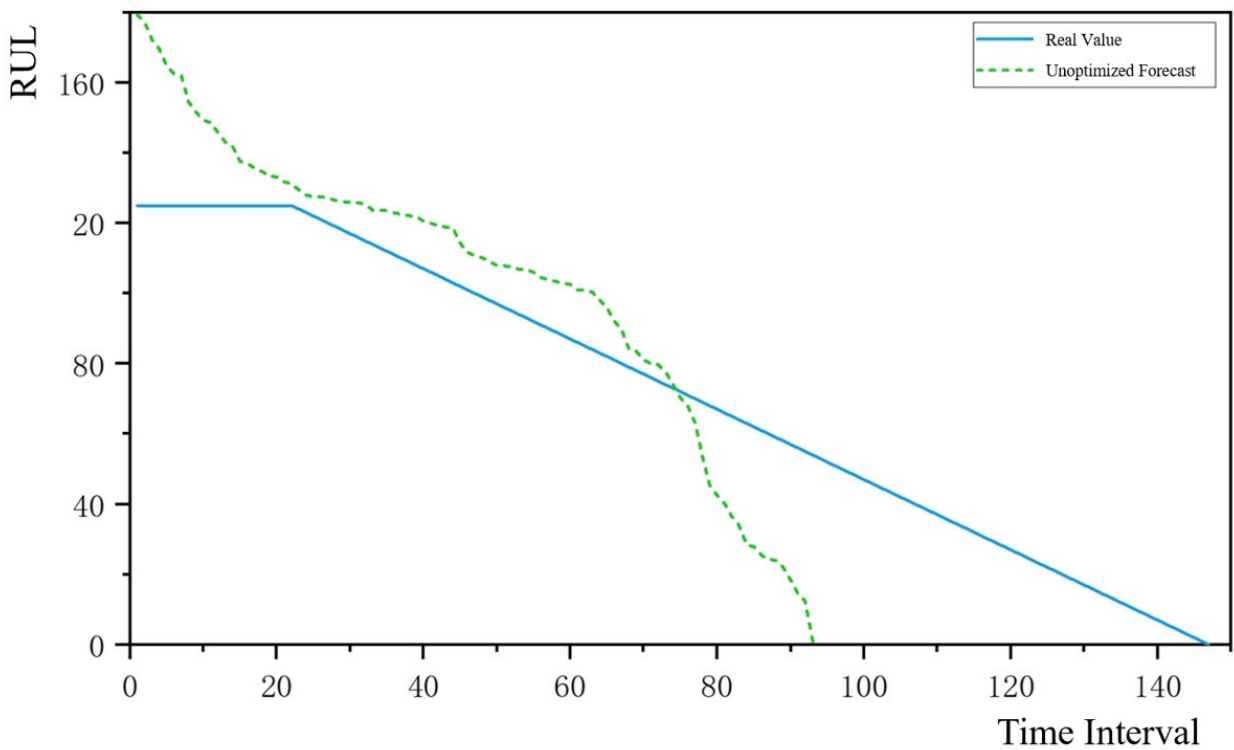


FIGURE 4. Preliminary model visualization.

once the dimensionality of the data input to the neural network is changed, the RMSE of RUL prediction results obtained after the training of LSTM and QPSO-LSTM networks will also vary. Therefore, the content of this chapter will be based on 15-dimensionality, and the FD001 subset of data will be downgraded step by step, aiming to obtain the optimal QPSO-LSTM performance degradation model.

The basic idea of the PCA algorithm is to map high-dimensional data in the low-dimensional space and maximize the retention of high-dimensional information in the low latitude projection space through the retention

of the main features of high-dimensional data, which is usually applied to the data preprocessing process of deep learning. In the PCA process, the selection of the number of principal components is extremely important, which is mainly determined by the value of the proportion of variance before and after projection.

Among them, the formula for the variance of the projected data is:

$$\text{Var}_{X_{\text{momid}}} = \sum_{j=1}^k J_j = \sum_{j=1}^k \lambda_j \quad (7)$$

Because the data are not changed by transforming the variance in different coordinate systems, the following is obtained:

$$\text{Var}_X = \text{Var}_{X_{\text{mint}}} = \sum_{j=1}^n J_j = \sum_{j=1}^n \lambda_j \quad (8)$$

Based on the above equation the selection of the number of principal components k can be carried out as expected:

$$\frac{\text{Var}_{X_{\text{project}}}}{\text{Var}_X} \geq q \quad (9)$$

where k is generally considered 0.99. The formula for calculating the minimum value of principal component quantity k is as follows:

$$\frac{\text{Var}_{X_{\text{project}}}}{\text{Var}_X} = \frac{\sum_{j=1}^k \lambda_j}{\sum_{j=1}^n \lambda_j} \geq 0.99 \quad (10)$$

Table 3 shows the histogram of the sequential data. The first column of the total significance is the eigenvalue of the male factor, the second column of the initial eigenvalue variance percentage indicates the degree of contribution of each male factor, and the last column is the sum of the eigenvalues of the second column. Usually, 90% is used as the threshold and the number of components used when the cumulative total reached 90% was used to determine the number of common factors to be extracted.

TABLE 3. Table of overall variance of data.

Ingredient	Total	Variance Percentage	Cumulative %
1	9.026	60.176	60.176
2	2.099	13.990	74.166
3	0.966	6.443	80.609
4	0.414	2.760	83.369
5	0.368	2.455	85.824
6	0.348	2.322	88.146
7	0.306	2.041	90.187
8	0.290	1.932	92.119
9	0.255	1.703	93.821
10	0.206	1.375	94.996
11	0.196	1.307	96.503
12	0.177	1.177	97.680
13	0.173	1.150	98.830
14	0.146	0.975	99.805
15	0.029	0.195	100.000

As shown in Table 3, downscaling to dimensions that are too low to fully express the remaining lifespan. In general, a data eigenvalue variance percentage of 90% was considered to be well expressed. In this chapter, to pursue a higher expression effect, 95% is used as the bottom line for the selection of dimensions, and finally 11 dimensions are selected as the lowest dimension. At the same time, in the research process of this chapter, the RMSE of the prediction results of each parameter combination in each dimension is obtained so that the comprehensive performance of the model of each dimension can be explored.

## B. MODEL PERFORMANCE OF INDIVIDUAL DIMENSION

### 1) 14-DIMENSION MODELS

The numerical RMSE performance of the 14-dimensional data model and its RMSE rankings related to the top ten data sets are listed in Tables 4 and Table 5 respectively.

In this chapter, 30 is used as the RMSE critical value, and it is considered that the sets of parameter sequences with RMSE values lower than 30 possess good prediction accuracy. There are a total of 15 sets in the 14-dimensional data model. Among them, there are three groups of parameters with RMSE values lower than 30, reaching 25.81, 27.82, and 27.89, respectively, accounting for 20% of all data combinations. The 14-dimensional model has a small amount of data, a large data variance, and average stability.

TABLE 4. Numerical performance of RMSE for 14-Dimensional data.

Minimum	Maximum	Average	Variance
25.81	65.06	43.57	185.34

TABLE 5. 14-Dimensional data RMSE top 10 parameter sequence related content.

Parameter Sequence	RMSE
S2,S3,S6:S9,S11:S15,S17,S20,S21	25.81
S2:S4,S6:S9,S12:S15,S17,S20,S21	27.82
S2:S4,S6:S9,S11,S13:S15,S17,S20,S21	27.98
S3,S4,S6:S9,S11:S15,S17,S20,S21	30.80
S2:S4,S6:S9,S11,S12,S14,S15,S17,S20,S21	33.99
S2:S4,S6:S9,S11:S13,S15,S17,S20,S21	34.96
S2:S4,S6:S9,S11:S15,S20,S21	37.24
S2:S4,S6,S7,S9,S11:S15,S20,S21	40.97
S2:S4,S7:S9,S11:S15,S17,S20,S21	42.92
S2:S4,S6:S8,S11:S15,S17,S20,S21	45.82

### 2) 13-DIMENSION MODELS

The numerical RMSE performance of the 13-dimensional data model and its RMSE rankings related to the top ten data sets are listed in Tables 6 and Table 7 respectively.

There were 105 groups in the 13-dimensional data model. Among them, a total of 12 sets of parameters had RMSE values lower than 30, reaching 24.70, 25.02, 25.43, 25.82, 26.76, 27.30, 28.10, 28.11, 28.52, 28.95, 29.15, and 29.27, which accounted for 11.43% of the total data combinations. The 13-dimensional data, compared to the 14-dimensional data, have a low variance, that is, greater overall model stability, but there are floating data with extremely high RMSE values.

TABLE 6. Numerical performance of RMSE for 13-Dimensional data.

Minimum	Maximum	Average	Variance
24.70	80.00	42.76	154.03

### 3) 12-DIMENSION MODELS

The numerical RMSE performance of the 12-dimensional data model and its RMSE rankings related to the

**TABLE 7. 13-Dimensional data RMSE top 10 parameter sequence related content.**

Parameter Sequence	RMSE
S2:S4,S6:S9,S12:S15,S20,S21	24.70
S2:S4,S6:S9,S11,S13,S14,S17,S20,S21	25.02
S2:S4,S6,S8,S9,S11:S15,S20,S21	25.43
S2:S4,S6,S8,S9,S11:S14,S17,S20,S21	25.82
S2,S3,S6,S7,S9,S11:S15,S17,S20,S21	26.76
S3,S4,S6:S9,S11:S14,S17,S20,S21	27.30
S2,S4,S6:S9,S12:S15,S17,S20,S21	28.10
S2:S4,S7,S8,S11:S15,S17,S20,S21	28.11
S2,S4,S6:S9,S11:S14,S17,S20,S21	28.52
S2,S4,S6:S9,S11:S15,S20,S21	28.95

top ten data sets are listed in Tables 8 and Table 9 respectively.

There were 455 groups in the 12-dimensional data model. A total of 72 sets of parameters had RMSE values lower than 30, accounting for 15.82% of all data combinations. The 12-dimensional data have a large variance, that is, the data are more volatile. However, there are numerous predictions with low RMSE values for the 12-dimensional data, although the maximum RMSE values are higher than those of the 13-dimensional and 14-dimensional data, and the overall performance is slightly prominent than that of the 14-dimensional and 13-dimensional data.

**TABLE 8. Numerical performance of RMSE for 12-Dimensional data.**

Minimum	Maximum	Average	Variance
22.79	85.82	37.84	170.88

**TABLE 9. 12-Dimensional data RMSE top 10 parameter sequence related content.**

Parameter Sequence	RMSE
S2:S4,S7,S9,S11:S13,S15,S17,S20,S21	22.79
S2:S4,S7:S9,S11,S13:S15,S20,S21	23.68
S2:S4,S7,S8,S11:S15,S17,S21	24.42
S2:S4,S6:S9,S11,S14,S17,S20,S21	24.67
S2:S4,S7:S9,S11,S13:S15,S17,S21	24.83
S2:S4,S7:S9,S11,S13:S15,S17,S20	24.84
S2,S4,S6,S8,S9,S11,S12,S14,S15,S17,S20,S21	24.95
S2:S4,S8,S11:S15,S17,S20	25.02
S2,S6:S9,S11:S14,S17,S20,S21	25.23
S2:S4,S7:S9,S11,S12,S14,S15,S17,S20	25.29

4) 11-DIMENSION MODELS

The numerical RMSE performance of the 11-dimensional data model and its RMSE rankings related to the top 10 data sets are listed in Tables 10 and Table 11 respectively.

The 11-dimensional data model had 1365 sets. A total of 92 sets of parameters had RMSE values lower than 30, accounting for 6.74% of all data combinations. The 11-parameter not only appeared to have the lowest RMSE prediction result of 22.04, but was also lower than the 12-dimensional data in terms of the maximum value and variance, which illustrates the characteristic of the model's strong stability in this dimension. However, the percentage of

parameter combinations with RMSE values lower than 30 for this dimensional model is lower than that of the previous two dimensions, with more than 50% of the combinations with RMSE values distributed within the [30,40] interval, and the overall performance is stable without a lack of prominent individuals.

**TABLE 10. Numerical performance of RMSE for 11-Dimensional data.**

Minimum	Maximum	Average	Variance
22.04	84.44	43.46	116.56

**TABLE 11. 11-Dimensional data RMSE top 10 parameter sequence related content.**

Parameter Sequence	RMSE
S3,S4,S7:S9,S11,S13:S15,S20,S21	22.04
S2:S4,S7,S9,S11:S13,S15,S20,S21	23.30
S3,S4,S8,S9,S11:S15,S17,S20	23.55
S2:S4,S7,S8,S11,S13:S15,S20,S21	23.68
S2:S4,S7:S9,S12,S14,S15,S20,S21	23.83
S2,S6:S9,S11:S15,S21	23.86
S3,S4,S7,S11:S15,S17,S20,S21	24.10
S3,S6:S9,S11:S15,S21	24.21
S3,S6:S9,S11:S15,S20	25.00
S3,S4,S6:S9,S12:S15,S21	25.01

C. OPTIMIZATION MODELING

1) OPTIMIZING RUL PREDICTION RESULTS

A total of eight sets of parameter combinations with RUL predicted RMSE values lower than 24, and their parameter combinations and RMSEs are listed in Table 12.

**TABLE 12. RMSE below 24 parameter combinations.**

Serial Number	Parameter Sequence	RMSE
1	S3,S4,S7:S9,S11,S13:S15,S20,S21	22.04
2	S2:S4,S7,S9,S11:S13,S15,S17,S20,S21	22.79
3	S2:S4,S7,S9,S11:S13,S15,S20,S21	23.30
4	S3,S4,S8,S9,S11:S15,S17,S20	23.55
5	S2:S4,S7,S8,S11,S13:S15,S20,S21	23.68
6	S2:S4,S7:S9,S11,S13:S15,S20,S21	23.68
7	S2:S4,S7:S9,S12,S14,S15,S20,S21	23.83
8	S2,S6:S9,S11:S15,S21	23.86

Fig.5 plots the results of the remaining life prediction against the top 2 ranked combinations of each parameter:

The RMSE of the 15-dimensional LSTM network remaining life prediction result is 38.57, and the RMSE of the QPSO-LSTM optimized network prediction result is 32.75. Compared with the unoptimized RUL prediction result, the RUL prediction result of the network optimized by the QPSO algorithm is improved by about 15%. Calculating the RMSE values of the LSTM prediction results of the top 8 parameter combinations and the corresponding RMSE values of the prediction results after QPSO, the parameter combinations from No. 1 to No. 8 are improved by 43.76%, 41.85%, 40.55%, 40.81%, 40.49%, 40.52%, 40.14%, and 40.04% respectively on the base model, which is much better than the initial modeling. far exceeds that of the preliminary modeling.



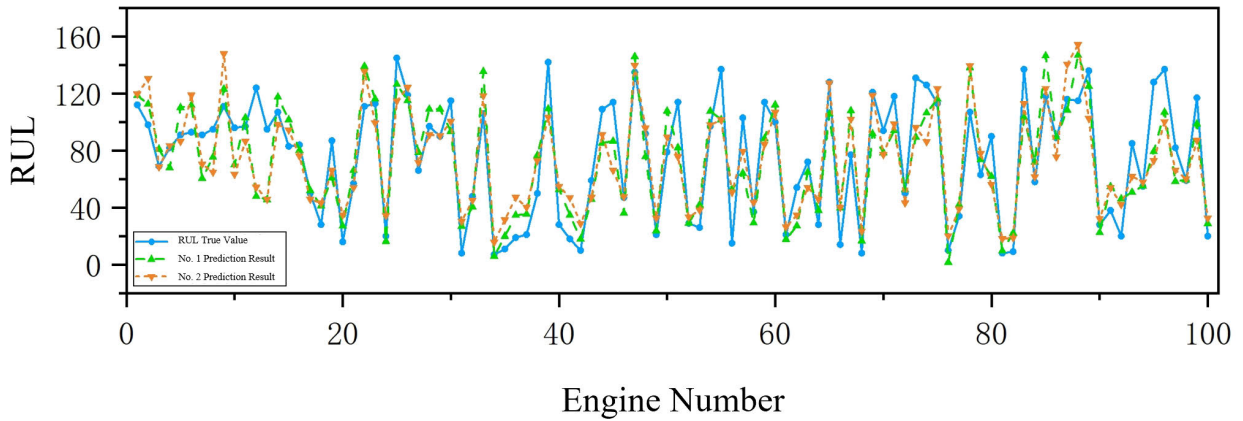


FIGURE 5. Plot of RUL prediction results against true values for parameter combinations no. 1-2.

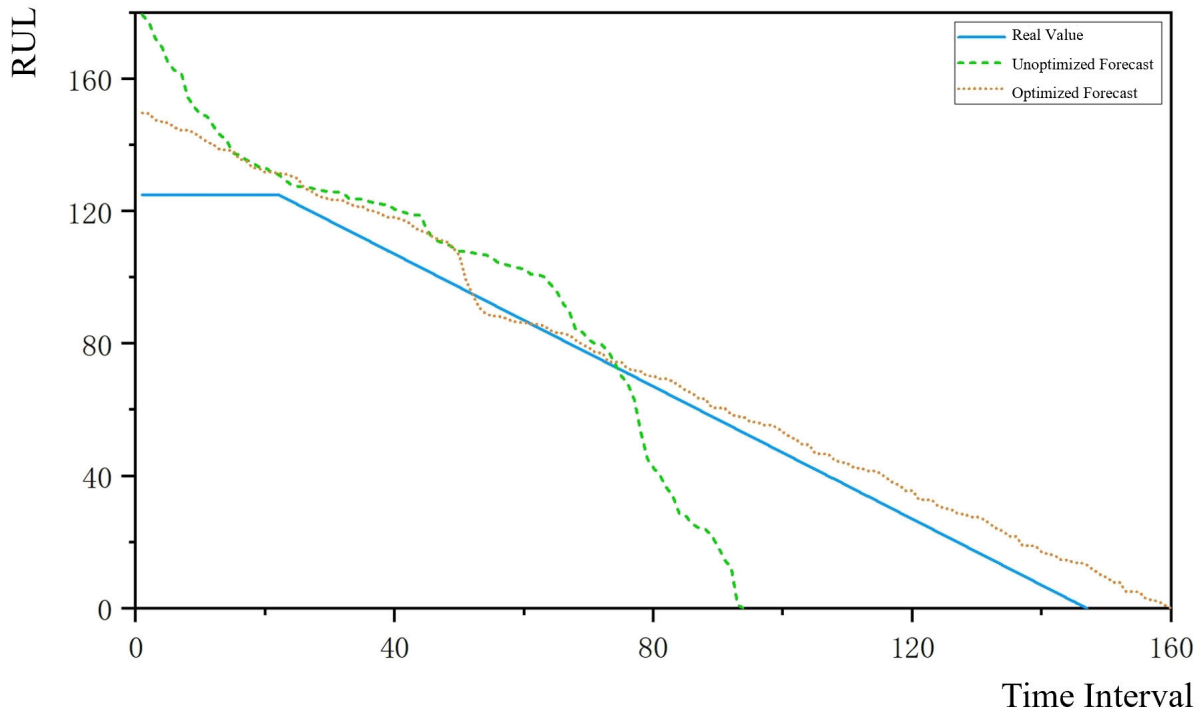


FIGURE 6. Plot of optimized aero-engine performance degradation model.

2) OPTIMIZING PERFORMANCE DEGRADATION MODELING RESULTS

The optimized performance degradation model was also established by considering engine No.2 in the FD001 subset of the C-MAPSS dataset as an example and comparing the optimized model with the preliminary model horizontally. The optimized aero-engine performance degradation model established for the parameter group ranked first in terms of RMSE value is shown in Fig.6. As can be seen from the figure below, although the optimized model does not match the trend of the real value at the initial time node, it presents an excellent linear fitting relationship after

crossing the threshold, and fits the real value very well in the middle of the RUL, although it deviates slightly with the decrease in the RUL. However, the overall performance is excellent, which greatly improves the performance of the initial model.

D. EXPANDED RESEARCH

1) OPTIMAL DIMENSIONAL ANALYSIS

To eliminate the magnitude, so that the various types of RMSE values change parameter side-by-side, this chapter on the parameters of the normalization process and, the results of the processing are shown in Figure.7. According to the

figure below, the 14-dimensional parameters of the variance, minimum value, mean value and ratio of superior value are ranked in the first four dimensions, while the maximum value is ranked at the bottom. The 13-dimensional parameter performance was very stable, and the parameters of the numerical rankings were in the second or third of the average position. 12-dimensional parameter is also ranked in the ratio of the superior value of the key factors in the ranking of the top; however, the mean value, variance, and maximum value are large, and the stability of this dimensional model is lacking. The 11-dimensional parameter variance was small, the mean value was small and the maximum value was large, and the stability of this dimensional model was not sufficient. The 11-dimensional parameter has a small variance and a large mean, and has the smallest RMSE value of the four dimensions. The RMSE value of the model fluctuates within a wide range, but does not have a significant minimum value or a good value share, and the overall performance is mediocre.

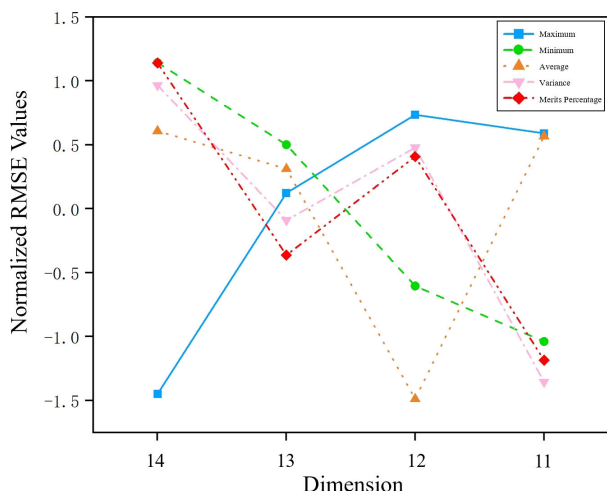


FIGURE 7. Normalized data trend overview chart.

Considering the performance of the four dimensional values, the 14- and 12-dimensional parameters perform more prominently, considering the small size of the 14-dimensional data and the inability to eliminate the random sampling error. In this section, the 12-dimensional parameter model is considered as the best dimension for QPSO-LSTM to establish an aero-engine performance degradation model.

2) SENSOR PARAMETER PERFORMANCE ANALYSIS

The excellent prediction results with the top ten RMSE values for each dimension were used to count the frequency of occurrence of each sensor parameter. Table 13 presents the statistical results.

According to Table 13, in the case of the total frequency of occurrence of 40, the frequency of occurrence of sensor No. S14 is as high as 38, that is, there are only two sets of preferred value parameter combinations without sensor no.S14, which can be observed to have a significant positive influence on the model, and the signal of this sensor represents the information

TABLE 13. Frequency statistics for each sensor parameter.

Parameter	Frequency
S2	32
S3	35
S4	35
S6	27
S7	36
S8	36
S9	36
S11	36
S12	33
S13	36
S14	38
S15	35
S17	27
S20	36
S21	35

of the converted speed of the core machine. In addition, sensors S7, S8, S9, S11, S13, and S20 appeared 36 times with the same frequency, demonstrating a positive influence. The sensor parameters S3, S4, S15, and S21 appeared 35 times and performed satisfactorily. It is worth noting that sensors S6 and S17 appeared only 27 times, which is less frequent than the other sensor signals, indicating that these two have poorer linearity level and more noise data, which is not significant for modeling positive influence modeling. Sensors S6 and S17 represent the total pressure of the engine’s outer culvert as well as the enthalpy of induced air, respectively.

Taken together, sensor signals S7, S8, S9, S11, S13, S14, and S20 have significant positive effects on the modeling of the QPSO-LSTM network, whereas sensors S2 and S12 have insignificant positive effects, and sensors S6 and S17 perform significantly poorly.

V. SUMMARY AND OUTLOOK

A. SUMMARY

With the rapid development of big data and artificial intelligence technology, the application of PHM technology in the real-time maintenance process of aero-engines have continued to make breakthroughs. The study of aero-engine performance degradation models based on sensor data is an important research direction of PHM technology, which is mainly aimed at ensuring the reliability and safety of aero-engine maintenance while achieving extremely high economic benefits that are difficult to realize by traditional periodic maintenance methods, and is an important part of the intelligent engine maintenance strategy. This project adopts a data-driven approach based on the C-MAPSS dataset as a data source, and provides a new methodology for establishing an aero-engine performance degradation model using the joint QPSO-LSTM algorithm.

The main work accomplished in this paper is as follows:

- After completing the three steps of data preprocessing, LSTM model building and QPSO algorithm optimization, this project successfully obtained the

aero-engine life prediction results and optimization prediction results based on the subset of the C-MAPSS dataset FD001. The RMSE value of the remaining life prediction result of the LSTM network was 38.57, and the RMSE value of the prediction result of the QPSO-LSTM optimization network was 32.75. In addition, the performance degradation model initially built by the combined QPSO-LSTM model fits the engine degradation model built by the segmented linear method generally well, especially in terms of the change of poles at the ends, and only roughly presents the engine degradation trend.

- To build a more reliable degradation model of aero-engine performance, further dimensionality reduction was performed on the dataset. Through this part of the study, it was found that the optimized parameters using the QPSO algorithm for tuning the LSTM network had a much better enhancement effect than the initial modeling. In particular, the optimized aero-engine performance degradation model built by the parameter group with the first ranked RMSE value, although it did not match the trend of the real value at the initial time node, showed an excellent linear fitting relationship after crossing the threshold, and the overall performance was excellent, which greatly improved the initial model performance.
- Based on the results of the dimensionality reduction experiments, it was found that the 12-dimensional parameter was the best dimension for QPSO-LSTM modeling, and the sensor signals of S7, S8, S9, S11, S13, S14, and S20 had a significant positive effect on the QPSO-LSTM network modeling, while the sensors of S6 and S17 had a mediocre performance.

## B. OUTLOOK

In this study, a data-driven approach based on a joint QPSO-LSTM network was successfully implemented to complete the remaining life prediction and performance degradation modeling for virtual data sets, which is of some value. However, for aero-engines, which are precise, complex and highly integrated mechanical devices, in-depth investigations and explorations are still needed to more accurately predict their remaining life and establish degradation curves with higher fitting performance.

The project has the following deficiencies:

- Due to the large number of parameter combinations involved in the dimensionality reduction process, only the FD001 subset of the C-MAPSS dataset was selected for the remaining life prediction and performance degradation model modeling in this project, and the next step of the work needs to comprehensively analyze the performance of each subset to improve the generalizability of the model.
- In the next step, modeling work using actual engine sensor data is considered.

## ACKNOWLEDGMENT

The authors would like to thank the Institute of Engineering Thermophysics, Chinese Academy of Sciences, National Key Laboratory of Science and Technology on Advanced Light-Duty Gas-Turbine for providing the hardware support needed to complete the project.

## REFERENCES

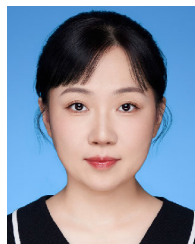
- [1] H. Huibing, "Research on reliability modeling and assessment method of performance degradation based on Bayesian updating and Copula theory," Southeast Univ., Dhaka, Bangladesh, Tech. Rep., 2016.
- [2] L. Guojian, "Research on data-driven prediction model of aero-engine performance degradation," Ph.D. dissertation, Civil Aviation Flight School China, Sichuan Province, China, 2023.
- [3] Y. M. Tao, "A review of classical artificial intelligence algorithms," *Softw. Guide*, vol. 19, no. 3, pp. 276–280, 2020.
- [4] H. Jiuyu, "Reliability analysis of aero-engine based on deep learning," Nanjing Univ. Aeronaut. Astronaut., Nanjing, China, Tech. Rep., 2019.
- [5] P. Xue, "Research on fault diagnosis and remaining life prediction of rotating machinery based on DBN," Yanshan Univ., Qinhuangdao, China, Tech. Rep., 2022.
- [6] L. Ren, Y. Sun, J. Cui, and L. Zhang, "Bearing remaining useful life prediction based on deep autoencoder and deep neural networks," *J. Manuf. Syst.*, vol. 48, pp. 71–77, Jul. 2018.
- [7] W. Hongfei, "Fault detection and remaining service life prediction of wind turbine bearings based on deep learning," Beijing Inst. Technol., Beijing, China, Tech. Rep., 2020.
- [8] C. Changchang, W. Huawei, N. Xiaomei, L. Ruiguan, and X. Minglan, "Residual life prediction of aircraft engines based on 1D-CNN and Bi-LSTM," *J. Mech. Eng.*, vol. 57, no. 14, pp. 304–312, 2021.
- [9] M. Zhong, G. Jiansheng, G. Taoyong, and M. Sheng, "Remaining life prediction of aircraft engine based on improved convolutional neural network," *J. Air Force Eng. Univ., Natural Sci. Ed.*, vol. 21, no. 6, pp. 19–25, 2020.
- [10] Z. Q. Chen, "Research on equipment health condition assessment and remaining life prediction method based on LSTM network," Ph.D. dissertation, Univ. Sci. Technol. China, Anhui, China, 2019.
- [11] Z. Huijie and G. Jiansheng, "Bidirectional LSTM neural network for aviation engine fault prediction," *J. Air Force Eng. Univ., Natural Sci. Ed.*, vol. 20, no. 4, pp. 26–32, 2019.
- [12] S. Vollert and A. Theissler, "Challenges of machine learning-based RUL prognosis: A review on NASA's C-MAPSS data set," in *Proc. 26th IEEE Int. Conf. Emerg. Technol. Factory Autom. (ETFA)*, Sep. 2021, doi: 10.1109/ETFA45728.2021.9613682.
- [13] L. Yong-Suo, M. Qing-Hua, C. Rong, W. Jian-Song, J. Shu-Min, and H. Yu-Zhu, "Improvement of similarity measure: Pearson product-moment correlation coefficient," *J. Chin. Pharmaceutical Sci.*, vol. 13, no. 3, pp. 180–186, 2004.
- [14] G. S. Babu, P. Zhao, and X. L. Li, "Deep convolutional neural network based regression approach for estimation of remaining useful life," in *Database Systems for Advanced Applications*. Cham, Switzerland: Springer, 2016.
- [15] C. Wrigley, "The distinction between common and specific variance in factor theory," *Brit. J. Stat. Psychol.*, vol. 10, no. 2, pp. 81–98, Nov. 1957.



**MINGYANG ZHOU** is currently pursuing the degree with the University of Chinese Academy of Sciences (UCAS), whose training unit is the Light-Duty Gas-Turbine Laboratory, Institute of Engineering Thermophysics. His research interests include fault diagnosis and fault-tolerant control of aero-engine control systems.



**KEQIANG MIAO** received the Ph.D. degree in aerospace propulsion theory and engineering from Beihang University, China, in 2023. Since then, he has been an Engineer with the Light-Duty Gas-Turbine Laboratory, Institute of Engineering Thermophysics, Chinese Academy of Sciences. His research interests include modeling and multi-variable control of aero engine and altitude ground test facilities.



**YAFENG SHEN** received the M.Sc. and Ph.D. degrees from Beijing Institute of Technology, in 2010 and 2020, respectively. She is currently a Senior Engineer with the Light-Duty Gas-Turbine Laboratory, Institute of Engineering Thermophysics, Chinese Academy of Sciences. Her research interests include the technologies for aero-engine health management, Intelligent control methods for aero-engines, and the development of aero-engine control and health management systems.



**JIAXIAN SUN** received the master's degree from the University of Chinese Academy of Sciences (UCAS), in 2022. She is currently an Engineer with the Light-Duty Gas-Turbine Laboratory, Institute of Engineering Thermophysics, Chinese Academy of Sciences. Her research interests include the development of control and health management systems for aero-engines and gas turbines.



**BO HAN** was born in 1986. He received the master's degree in engineering from Beijing Jiaotong University, China, in 2012. From 2012 to 2016, he was with AVIC Beijing Shuguang Aviation Electric Company Ltd., engaged in the research and development of the design and software implementation of the aero-generator controller. From 2016 to 2021, he was a Senior Engineer with the Light-Duty Gas-Turbine Laboratory, Institute of Engineering Thermophysics, Chinese Academy of Sciences. As the project leader, he presided more than several research projects, such as national major projects and innovation projects of the Science and Technology Commission. He mainly engaged in aero engine/gas turbine control algorithm and strategy research, control system research and development, undertaking the laboratory military model engine electronic controller development and finalize work, and enterprise cooperation projects. During his tenure, he presided more than the development and identification of the first military-grade turbofan engine controller of the Chinese Academy of Sciences, and several types of engine electronic controllers developed have been flight verifiers. A good accumulation has been owned in the design and testing of aero-engine electronic controllers. In 2020, he won the first prize of the Military Science and Technology Progress.

...